Mathematical assessment of the roles of vaccination and non-pharmaceutical interventions on COVID-19 dynamics: a multigroup modeling approach

Abba B. Gumel[†,††] [*], Enahoro A. Iboi[◇], Calistus N. Ngonghala[‡,‡‡] and Gideon A. Ngwa[†††]

[†] *School of Mathematical and Statistical Sciences, Arizona State University, Tempe, Arizona, 85287, USA.*

[◇] *Department of Mathematics, Spelman College, Atlanta, Georgia, 30314, USA.*

[‡] *Department of Mathematics, University of Florida, Gainesville, FL 32611, USA.*

[‡‡] *Emerging Pathogens Institute, University of Florida, Gainesville, FL 32610, USA.*

[††] *Department of Mathematics and Applied Mathematics, University of Pretoria, Pretoria 0002, South Africa.*

[†††] *Department of Mathematics, University of Buea, P.O. Box 63, Buea, Cameroon.*

Abstract

A novel coronavirus emerged in December of 2019 (COVID-19), causing a pandemic that continues to inflict unprecedented public health and economic burden in all nooks and corners of the world. Although the control of COVID-19 has largely focused on the use of basic public health measures (primarily based on using non-pharmaceutical interventions, such as quarantine, isolation, social-distancing, face mask usage and community lockdowns), a number of exceptionally-promising vaccines are about to be approved for use in humans by the U.S. Food and Drugs Administration. We present a new mathematical model for assessing the population-level impact of the candidate vaccines, particularly for the case where the vaccination program is complemented with a social-distancing control measure at a certain compliance level. The model stratifies the total population into two subgroups, based on whether or not they habitually wear face mask in public. The resulting multigroup model, which takes the form of a compartmental, deterministic system of nonlinear differential equations, is parametrized using COVID-19 cumulative mortality data. Conditions for the asymptotic stability of the associated disease-free equilibrium, as well as expression for the vaccine-derived herd immunity threshold, are derived. This study shows that the prospect of COVID-19 elimination using any of the three candidate vaccines is quite promising, and that such elimination is more feasible if the vaccination program is combined with social-distancing control measures (implemented at moderate to high level of compliance).

Keywords: *COVID-19; vaccine; social-distancing; herd immunity; face mask; stability; reproduction number.*

1 Introduction

The novel coronavirus (COVID-19) pandemic, which started as a pneumonia of an unknown etiology late in December 2019 in the city of Wuhan, is the most devastating public health challenge mankind has faced since the 1918/1919 pandemic of influenza. The COVID-19 pandemic, which rapidly spread to essentially every nook and corner of the planet, continues to inflict devastating public health and economic challenges globally. As of December 5, 2020, the pandemic accounts for $67,021,834$ confirmed cases and $1,537,165$ cumulative mortality globally. Similarly, the United States, which recorded its first COVID-19 case on January 20, 2020, recorded $14,991,531$ confirmed cases and $287,857$ deaths (as of December 5, 2020) [1].

COVID-19, a member of the Coronavirus family of RNA viruses that cause diseases in mammals and birds, is primarily transmitted from human-to-human through direct contact with contaminated objects or surfaces and through inhalation of respiratory droplets from both symptomatic and asymptomatically-infectious humans (*albeit* there is limited evidence that COVID-19 can be transmitted *via* exhalation through normal breathing and aerosol [2]. The incubation period of the disease is estimated to lie between 2 to 14 days (with a mean of 5.1 days), and majority

[*]Corresponding author: Email: *agumel@asu.edu*

of individuals infected with the disease show mild or no clinical symptoms [3]. The symptoms typically include coughing, fever and shortness of breadth (for mild cases) and pneumonia for severe cases [3]. The people most at risk of dying from, or suffering severe illness with, COVID-19 are those with co-morbidities (such as individuals with diabetes, obesity, kidney disease, cardiovascular disease, chronic respiratory disease etc.). Younger people, front line healthcare workers and employees who maintain close contacts (within 6 feet) with customers and other co-workers (such as meat factory workers, retail store workers etc.) are also at risk.

Although there are three exceptionally-promising candidate vaccines (by Pfizer, Inc., Moderna, Inc. and AstraZeneca, Inc.) and antivirals undergoing various stages of development (Pfizer has filed for FDA Emergency Use Authorization on November 20, 2020) [4], there is currently no safe and effective vaccine or antiviral that has been approved for widespread use in humans, *albeit* the approval of the aforementioned candidate vaccines is imminently expected by the end of 2020. Further, owing to its limited supply, the approved anti-COVID drug *remdesivir* is limited for use to treat individuals in hospital who display severe symptoms of COVID-19. Hence, due to the absence of safe and effective vaccines and antiviral for widespread use in humans, efforts to control and mitigate the burden of COVID-19 remain focused on non-pharmaceutical interventions (NPIs), such as quarantine, self-isolation, social (physical) distancing, the use of face masks in public, hand washing (with approved sanitizers), community lockdowns, testing and contact tracing. Of these NPIs, the use of face masks in public is considered to be the main mechanism for effectively curtailing COVID-19 [3, 5–7].

The Pfizer and Moderna vaccines, each of estimated protective efficacy of about 95% [4, 8, 9], are genetic vaccines that are developed based on stimulating a mechanism that encourages the body to produce antibodies that fights the SARS-CoV-2. Specifically, the vaccines use a synthetic messenger RNA (*m*RNA) that carries instructions for making virus spike protein to gain entry into cells when injected into muscle tissue in the upper arm. This triggers the immune system to recognize the spike protein and develop antibodies against it (so that when a human is infected with SARS-CoV-2, his/her body is able to successfully fight it) [4, 10]. Two doses are required for both the Pfizer and Moderna vaccine candidates (one to prime the immune system, and the second to boost it). For the Pfizer vaccine, the second dose will be administered 19-42 days after the first dose. The second dose of the Moderna vaccine is administered three to four weeks after the first dose. Both vaccines need to be stored at appropriate refrigeration temperatures [11]. The AstraZeneca vaccine, on the other hand, has estimated protective efficacy of 70% [4, 8, 9]. It uses a replication-deficient chimpanzee viral vector that causes infections in chimpanzees and contains the genetic material of the SARS-CoV-2 virus spike protein [9]. When injected into the human, the spike protein triggers the immune system to attack the SARS-CoV-2 virus that infects the body [9]. AstraZeneca vaccine also requires two doses (one month apart) to achieve immunity, and, unlike the Pfizer and Moderna vaccines, does not have to be stored in super-cold temperatures (it can be stored at normal refrigerated temperature of (2-8$^{\circ}C$) for at least six months) [9]. Hence, owing to the imminence for the approval of the aforementioned three candidate COVID-19 vaccines by the FDA, coupled with the primary role of face masks usage, it is instructive to design new mathematical models that will allow for the realistic assessment of the combined impact of the expected COVID-19 vaccines and face masks usage in a community.

Numerous mathematical models, of various types, have been developed and used to provide insight into the transmission dynamics and control of COVID-19. The modeling types used include statistical [12], compartmental/deterministic (e.g., [3, 5–7, 13]), stochastic (e.g., [14, 15]), network (e.g., [16]) and agent-based (e.g., [17]). The purpose of the current study is to use mathematical modeling approaches, coupled with mathematical and statistical data analytics, to assess the combined impact of the expected COVID-19 vaccines and face masks usage. A notable feature of the model to be developed is its multigroup nature. Specifically, the total population will be subdivided into two groups, namely those who habitually wear face mask in public and those who do not. Data for COVID-19 pandemic in the U.S. will be used to parametrize the model. The central goal of the study is to determine the minimum vaccine coverage level needed to effectively curtail (or eliminate) community transmission of COVID-19 in the U.S., and to quantify the reduction in the required vaccine coverage if the vaccination program is supplemented with face masks usage (under various face masks efficacy and compliance parameter space). The paper is organized as follows. The novel multigroup model is formulated in Section 2. The parameters of the model are also estimated, based on fitting the model with U.S. COVID-19 data. The model is rigorously analysed, with respect to the asymptotic stability of the disease-free equilibrium of the model, in Section 3. A condition for

achieving community-wide vaccine-derived herd immunity is also derived. Numerical simulations of the model are reported in Section 4. Discussions and concluding remarks are presented in Section 5.

2 Formulation of Mathematical Model

In order to account for heterogeneity in face masks usage in the community, the total population of individuals in the community at time t, denoted by $N(t)$, is split into the total sub-populations of individuals who do not habitually wear face mask in public (labeled "*non-mask users*"), denoted by $N_1(t)$, and the total sub-populations of those who habitually wear face mask in public (labeled "*mask users*"), represented by $N_2(t)$. That is, $N(t) = N_1(t) + N_2(t)$. Furthermore, the sub-population $N_1(t)$ is sub-divided into the mutually-exclusive compartments of unvaccinated susceptible ($S_{1u}(t)$), vaccinated susceptible ($S_{1v}(t)$), exposed ($E_1(t)$), pre-symptomatically-infectious ($P_1(t)$), symptomatically-infectious ($I_1(t)$), asymptomatically-infectious ($A_1(t)$), hospitalized ($H_1(t)$) and recovered ($R_1(t)$) individuals, so that

$$N_1(t) = S_{1u}(t) + S_{1v}(t) + E_1(t) + P_1(t) + I_1(t) + A_1(t) + H_1(t) + R_1(t).$$

Similarly, the total sub-population of the mask users, $N_2(t)$, is stratified into the compartments for unvaccinated susceptible ($S_{2u}(t)$), vaccinated susceptible ($S_{2v}(t)$), exposed ($E_2(t)$), pre-symptomatically-infectious ($P_2(t)$), symptomatically-infectious ($I_2(t)$), asymptomatically-infectious ($A_2(t)$), hospitalized ($H_2(t)$) and recovered ($R_2(t)$) individuals. Hence,

$$N_2(t) = S_{2u}(t) + S_{2v}(t) + E_2(t) + P_2(t) + I_2(t) + A_2(t) + H_2(t) + R_2(t).$$

The equations for the rate of change of the sub-populations of non-mask users is given by the following deterministic system of nonlinear differential equations (where a dot represents differentiation with respect to time t):

$$\begin{aligned}
\dot{S}_{1u} &= \Pi + \omega_v S_{1v} + \alpha_{21} S_{2u} - \lambda_1 S_{1u} - (\alpha_{12} + \xi_v + \mu) S_{1u}, \\
\dot{S}_{1v} &= \xi_v S_{1u} + \alpha_{21} S_{2v} - (1-\varepsilon_v)\lambda_1 S_{1v} - (\alpha_{12} + \omega_v + \mu) S_{1v}, \\
\dot{E}_1 &= \lambda_1 S_{1u} + (1-\varepsilon_v)\lambda_1 S_{1v} + \alpha_{21} E_2 - (\alpha_{12} + \sigma_1 + \mu) E_1, \\
\dot{P}_1 &= \sigma_1 E_1 + \alpha_{21} P_2 - (\alpha_{12} + \sigma_P + \mu) P_1, \\
\dot{I}_1 &= r\sigma_P P_1 + \alpha_{21} I_2 - (\alpha_{12} + \phi_{1I} + \gamma_{1I} + \mu + \delta_{1I}) I_1, \\
\dot{A}_1 &= (1-r)\sigma_P P_1 + \alpha_{21} A_2 - (\alpha_{12} + \gamma_{1A} + \mu) A_1, \\
\dot{H}_1 &= \phi_{1I} I_1 + \alpha_{21} H_2 - (\alpha_{12} + \gamma_{1H} + \mu + \delta_{1H}) H_1, \\
\dot{R}_1 &= \gamma_{1I} I_1 + \gamma_{1A} A_1 + \gamma_{1H} H_1 + \alpha_{21} R_2 - (\alpha_{12} + \mu) R_1,
\end{aligned} \tag{2.1}$$

where, λ_1 is the *force of infection*, defined by:

$$\lambda_1 = (1 - c_s)\left[\frac{(\beta_{P_1} P_1 + \beta_{I_1} I_1 + \beta_{A_1} A_1 + \beta_{H_1} H_1)}{N_1} + (1-\varepsilon_o)\frac{(\beta_{P_2} P_2 + \beta_{I_2} I_2 + \beta_{A_2} A_2 + \beta_{H_2} H_2)}{N_2}\right],$$

with $\beta_i \, \{i = P_1, I_1, A_1, H_1, P_2, I_2, A_2 \text{ and } H_2\}$ the effective contact rate for individuals in the respective $P_1, I_1, A_1, H_1, P_2, I_2, A_2$ and H_2 classes. The parameters $0 < \varepsilon_o < 1$ and $0 < \varepsilon_i < 1$ represent the outward and inward protective efficacy, respectively, of face masks to prevent the transmission of infection to a susceptible individual (ε_o) as well as prevent the acquisition of infection (ε_i) from an infectious individual, while $0 \leq c_s < 1$ is a parameter that accounts social-distancing compliance.

In (2.1), the parameter Π is the recruitment (birth or immigration) rate of individuals into the population, α_{21} is the rate of change of behavior for non-habitual face masks users to become habitual users (i.e., α_{12} is the transition rate from group 2 to group 1). Furthermore, α_{12} is the rate at which habitual face masks users choose to be non-habitual wearers. The parameter ξ_v represents the vaccination rate, and the vaccine is assumed to induce protective

efficacy $0 < \varepsilon_v < 1$ in all vaccinated individuals and wane at a rate ω_v. Natural deaths occurs in all epidemiological classes at a rate μ. Individuals in the E_1 class progress to the pre-symptomatic stage at a rate σ_1, and those in the pre-symptomatic class (P_1) transition out of this class at a rate σ_P (a proportion, q, of which become symptomatic, and move to the I class at a rate $q\sigma_P$, and the remaining proportion, $1-q$, move to the asymptomatically-infectious class at a rate $(1-q)\sigma_P$). Symptomatic infectious individuals are hospitalized at a rate ϕ_{1I}. They recover at a rate γ_{1I} and die due to the disease at a rate δ_{1I}. Hospitalized individuals die of the disease at the rate δ_{1H}.

Similarly, the equations for the rate of change of the sub-populations of mask users is given by:

$$\begin{aligned}
\dot{S}_{2u} &= \omega_v S_{2v} + \alpha_{12} S_{1u} - \lambda_2 S_{2u} - (\alpha_{21} + \xi_v + \mu) S_{2u}, \\
\dot{S}_{2v} &= \xi_v S_{2u} + \alpha_{12} S_{1v} - (1-\varepsilon_v)\lambda_2 S_{2v} - (\alpha_{21} + \omega_v + \mu) S_{2v}, \\
\dot{E}_2 &= \lambda_2 S_{2u} + (1-\varepsilon_v)\lambda_2 S_{2v} + \alpha_{12} E_1 - (\alpha_{21} + \sigma_2 + \mu) E_2, \\
\dot{P}_2 &= \sigma_2 E_2 + \alpha_{12} P_1 - (\alpha_{21} + \sigma_P + \mu) P_2, \\
\dot{I}_2 &= q\sigma_P P_2 + \alpha_{12} I_1 - (\alpha_{21} + \phi_{2I} + \gamma_{2I} + \mu + \delta_{2I}) I_2, \\
\dot{A}_2 &= (1-q)\sigma_P P_2 + \alpha_{12} A_1 - (\alpha_{21} + \gamma_{2A} + \mu) A_2, \\
\dot{H}_2 &= \phi_{2I} I_2 + \alpha_{12} H_1 - (\alpha_{21} + \gamma_{2H} + \mu + \delta_{2H}) H_2, \\
\dot{R}_2 &= \gamma_{2I} I_2 + \gamma_{2A} A_2 + \gamma_{2H} H_2 + \alpha_{12} R_1 - (\alpha_{21} + \mu) R_2,
\end{aligned} \tag{2.2}$$

where,

$$\lambda_2 = (1-c_s)(1-\varepsilon_i)\left[\frac{(\beta_{P_1} P_1 + \beta_{I_1} I_1 + \beta_{A_1} A_1 + \beta_{H_1} H_1)}{N_1} + (1-\varepsilon_o)\frac{(\beta_{P_2} P_2 + \beta_{I_2} I_2 + \beta_{A_2} A_2 + \beta_{H_2} H_2)}{N_2}\right].$$

Thus, Equations (2.1) and (2.2) represent the multi-group model for assessing the population impact of face masks usage and vaccination on the transmission dynamics and control of COVID-19 in a community. The flow diagram of the model $\{(2.1), (2.2)\}$ is depicted in Figure 1 (the state variables and parameters of the model are described in Tables 5 and 6, respectively).

Some of the main assumptions made in the formulation of the multi-group model $\{(2.1), (2.2)\}$ include the following:

1. Homogeneous mixing (i.e., we assumed a well-mixed population, where every member of the community is equally likely to mix with every other member of the community).

2. Exponentially-distributed waiting time in each epidemiological compartment.

3. The anti-COVID vaccine is imperfect. That is, the vaccine offers partial protective immunity (with efficacy $0 < \varepsilon_v < 1$), which wanes over time (at a rate ω_v). Further, it is assumed that the vaccine does not offer any therapeutic benefit (such as slowing progression to active disease or increasing recovery rate in breakthrough infections). It is also assumed that individuals in the vaccinated class received all the required doses of the vaccine, and that the vaccine has been stored under the prescribed temperature conditions.

4. Although there is currently no definitive data on the level (partial or complete) and duration of COVID-19 immunity due to recovery from infection, we assume that natural recovery from infection confers permanent immunity against reinfection. Further, successfully-immunized individuals (i.e., individuals who acquired vaccine-derived immunity) remain in the vaccinated class (rather than moved to the recovered class).

5. Endemicity assumption: although epidemic models (with no demographics) are typically used for studying the dynamics of new epidemics, such as COVID-19, we assume that, for the purpose of vaccination program, COVID-19 has attained endemic status. This is to account for the fact that the vaccine will be administered to every member of the community (including newborns) for an extended period of time (perhaps years).

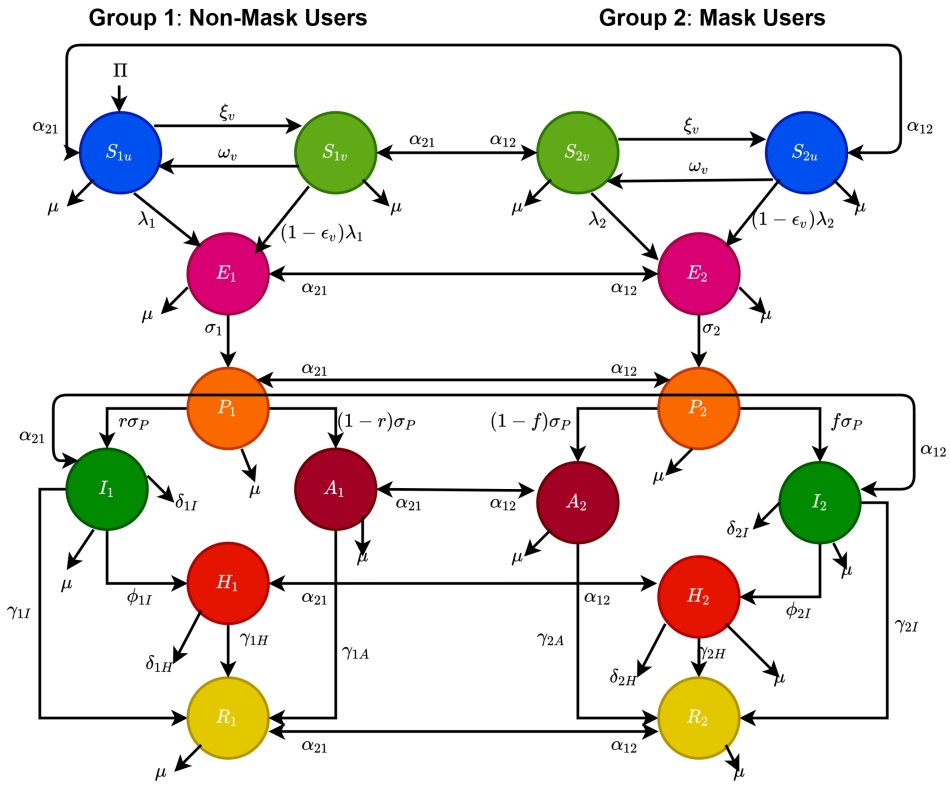

Figure 1: Flow diagram of the model $\{(2.1), (2.2)\}$.

The implication of this assumption is that human demography (as represented by the recruitment parameter, Π, and the natural death parameter, μ) must be incorporated into the model.

The multi-group model $\{(2.1), (2.2)\}$ is an extension of the two-group mask-use model in [5] by, *inter alia*:

(i) allowing for back-and-forth transitions between the two groups (mask-users and non-mask-users), to account for human behavioral changes *vis a vis* decision to either be (or not to be) a face mask user in public;

(ii) incorporating an imperfect vaccine, which offers protective efficacy ($0 < \varepsilon_v < 1$) against acquisition of COVID-19 infection, which may wane over time (at a rate ω_v);

(iii) allowing for disease transmission by pre-symptomatic and asymptomatically-infectious individuals.

2.1 Data Fitting and Parameter Estimation

In this section, cumulative mortality data for the US (from January 22, 2020 to November 16, 2020) will be used to fit the model (2.1)-(2.2) in the absence of vaccination and estimate some of its key parameters. In particular, the parameters to be estimated from the data are the community transmission rate for individuals who do not wear face masks in public (β_1), the transmission rate for individuals who habitually wear face masks in public (β_2), the inward efficacy of masks in preventing disease acquisition by susceptible individuals who habitually wear face masks (ε_i), the outward efficacy of masks to prevent the spread of disease by infected individuals who habitually wear face masks (ε_o), the proportion of individuals in the community who comply to social-distancing measures while in public (c_s), the rate at which people who do not wear masks adopt a mask-wearing habit (α_{12}), the rate at which those who habitually wear face masks stop wearing masks in public (α_{21}), and the mortality rates of symptomatic infectious and hospitalized individuals (δ_i and δ_h, respectively). It should be mentioned that modification parameters η_P, η_I, η_A, and η_H relating to disease transmission by pre-symptomatic infectious, symptomatic infectious, asymptomatic infectious and hospitalized individuals, respectively, are introduced in the

forces of infection λ_1 and λ_2, so that $\beta_j = \eta_j \beta_k$ ($j \in \{P_k, I_k, A_k, H_k\}, k \in \{1, 2\}$). The model fitting was carried out using MATLAB R2020b and the process involved minimizing the sum of the square differences between each observed cumulative mortality data point and the corresponding mortality point obtained from the model (2.1)-(2.2) in the absence of vaccination [3, 18, 19]. The choice of mortality over case data is motivated by the fact that mortality data for COVID-19 is more reliable than case data (see [6] for details). The estimated values of the fitted parameters are tabulated in Table 1(a). The fitting of the model to the observed cumulative and daily mortality data is depicted in Figure 2 (a). Furthermore, Figure 2 (b) compares the simulations of the model using the fitted (estimated) and fixed parameters (given in Tables 1 (a) and (b)-(c)) with the observed daily COVID-19 mortality for the US, showing a good fit.

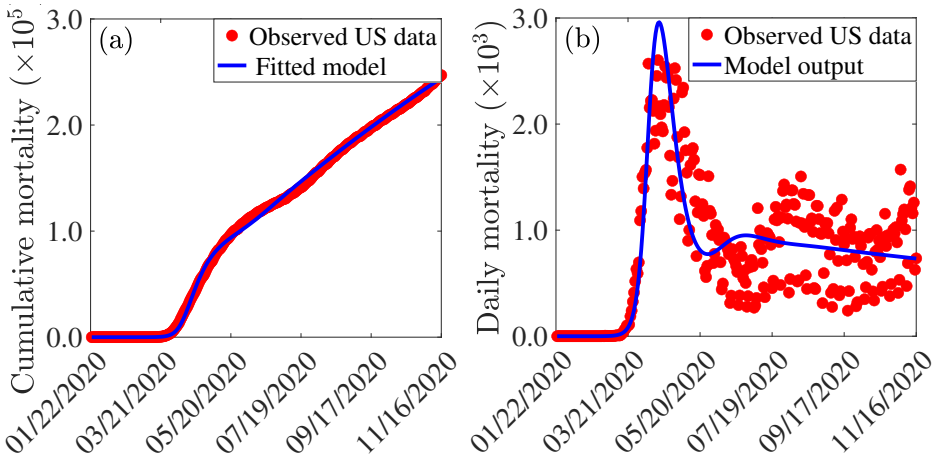

Figure 2: (a) Observed cumulative mortality data for the US (red dots) and predicted cumulative mortality for the US from the model (2.1)-(2.2) (with no vaccination) for the period from January 22 to November 16, 2020. (b) Simulations of the model (2.1)-(2.2) using the fixed parameters in Table 1(b)-(c) and the estimated parameters from the cumulative COVID-19 mortality data for the US presented in Table 1(a). We started the simulations of the pandemic near the disease-free equilibrium for the US. In particular, we used the following initial conditions (with mask usage compliance initially set at 1% of the total current US population): $(S_1^0, E_1^0, P_1^0, I_1^0, A_1^0, H_1^0, R_1^0, S_2^0, E_2^0, P_2^0, I_2^0, A_2^0, H_2^0, R_2^0) = (0.99 \times 336218660 - 1, 0, 0, 1, 0, 0, 0, 0.01 \times 336218660, 0, 0, 0, 0, 0, 0)$.

Table 1: Baseline parameter values for the model (2.1)-(2.2). (a) Estimated (fitted) parameter values for the model in the absence of vaccination, using COVID-19 mortality data for the US for the period from January 22, 2020 to November 16, 2020. (b)-(c) Baseline values of the remaining fixed parameters of the model (2.1)-(2.2) extracted from the literature or estimated using information from the literature.

(a) Fitted parameters

Parameter	Value
β_1	0.6566/day
β_2	0.5249/day
c_s	0.3051
ε_o	0.6304
ε_i	0.9965
α_{12}	0.0459/day
α_{21}	0.0010/day
δ_i	0.0008/day
δ_h	0.0025/day

(b) Fixed parameters

Parameter	Value	Source
σ_1	$1/2.5$/day	[20, 21]
σ_2	$1/2.5$/day	[20, 21]
σ_p	$1/2.5$/day	[20, 21]
r (q)	0.2(0.2)	[22, 23]
ϕ_{1I}	$1/6$/day	[24]
ϕ_{2I}	$1/6$/day	[24]
γ_I	$1/10$/day	[17, 25]
γ_A	$1/5$/day	[24]
γ_H	$1/8$/day	[17]

(c) Fixed parameters

Parameter	Value	Source
Π	1.2×10^4/day	Estimated
μ	$1/(79 \times 365)$/day	Estimated
η_P	1.25	Assumed
η_I	1.0	Assumed
η_A	1.50	Assumed
η_H	0.25	Assumed
ω_v	0/day	Assumed
ξ_v	2.97×10^{-4}/day	Assumed
ε_v	0.70	[8, 9]

3 Mathematical Analysis

Since the model $\{(2.1), (2.2)\}$ monitors the temporal dynamics of human populations, all state variables and parameters of the model are non-negative. Consider the following biologically-feasible region for the model:

$$\Omega = \left\{ (S_{1u}, S_{1v}, S_{2u}, S_{2v}, E_1, E_2, P_1, P_2, I_1, I_2, A_1, A_2, H_1, H_2, R_1, R_2) \in \mathbf{R}_+^{16} : N(t) \leq \frac{\Pi}{\mu} \right\}. \tag{3.1}$$

Theorem 3.1. *The region Ω is positively-invariant with respect to the model $\{(2.1), (2.2)\}$.*

Proof. Adding all the equations of the model $\{(2.1), (2.2)\}$ gives

$$\dot{N} = \Pi - \mu N - \delta_{1I} I_1 - \delta_{1H} H_1 - \delta_{2I} I_2 - \delta_{2H} H_2. \tag{3.2}$$

Recall that all parameters of the model $\{(2.1), (2.2)\}$ are non-negative. Thus, it follows, from (3.2), that

$$\dot{N} \leq \Pi - \mu N. \tag{3.3}$$

Hence, if $N > \frac{\Pi}{\mu}$, then $\dot{N} < 0$. Furthermore, by applying a standard comparison theorem [26] on (3.3), we have:

$$N(t) \leq N(0)e^{-\mu t} + \frac{\Pi}{\mu}(1 - e^{-\mu t}).$$

In particular, $N(t) \leq \frac{\Pi}{\mu}$ if $N(0) \leq \frac{\Pi}{\mu}$. Thus, every solution of the model $\{(2.1), (2.2)\}$ with initial conditions in Ω remains in Ω for all time $t > 0$. In other words, the region Ω is positively-invariant and attracts all initial solutions of the model $\{(2.1), (2.2)\}$. Hence, it is sufficient to consider the dynamics of the flow generated by $\{(2.1), (2.2)\}$ in Ω (where the model is epidemiologically- and mathematically well-posed) [27]. □

3.1 Asymptotic Stability of Disease-free Equilibrium

The model $\{(2.1), (2.2)\}$ has a unique disease-free equilibrium (DFE), obtained by setting all the infected compartments of the model to zero, (where $S_{1u}^* > 0$, $S_{1v}^* > 0$, $S_{2u}^* > 0$ and $S_{2v}^* > 0$; their expressions are too lengthy, hence not presented here)

$$\mathbb{E}_0 : \ (S_{1u}^*, S_{1v}^*, S_{2u}^*, S_{2v}^*, E_1^*, E_2^*, P_1^*, P_2^*, I_1^*, I_2^*, A_1^*, A_2^*, H_1^*, H_2^*, R_1^*, R_2^*) =$$

$$\left(\frac{\Pi + \omega_v S_{1v}^* + \alpha_{21} S_{2u}^*}{\alpha_{12} + \xi_v + \mu}, \ \frac{\xi_v S_{1u}^* + \alpha_{21} S_{2v}^*}{\alpha_{12} + \omega_v + \mu}, \frac{\omega_v S_{2v}^* + \alpha_{12} S_{1u}^*}{\alpha_{21} + \xi_v + \mu}, \frac{\xi_v S_{2u}^* + \alpha_{12} S_{1v}^*}{\alpha_{21} + \omega_v + \mu}, 0, 0, 0, 0, 0, 0, 0, 0, 0, 0, 0, 0 \right).$$

The local asymptotic stability property of the DFE ($\mathbb{E}_0$) can be explored using the *next generation operator* method [28, 29]. In particular, using the notation in [28], it follows that the associated non-negative matrix (F) of new infection terms, and the M-matrix (V), of the linear transition terms in the infected compartments, are given, respectively, by (where the entries f_i and g_i, $i = 1, \cdots, 8$, of the non-negative matrix F, are given in Appendix I):

$$F = \begin{bmatrix} 0 & f_1 & f_2 & f_3 & f_4 & 0 & f_5 & f_6 & f_7 & f_8 \\ 0 & 0 & 0 & 0 & 0 & 0 & 0 & 0 & 0 & 0 \\ 0 & 0 & 0 & 0 & 0 & 0 & 0 & 0 & 0 & 0 \\ 0 & 0 & 0 & 0 & 0 & 0 & 0 & 0 & 0 & 0 \\ 0 & 0 & 0 & 0 & 0 & 0 & 0 & 0 & 0 & 0 \\ 0 & g_1 & g_2 & g_3 & g_4 & 0 & g_5 & g_6 & g_7 & g_8 \\ 0 & 0 & 0 & 0 & 0 & 0 & 0 & 0 & 0 & 0 \\ 0 & 0 & 0 & 0 & 0 & 0 & 0 & 0 & 0 & 0 \\ 0 & 0 & 0 & 0 & 0 & 0 & 0 & 0 & 0 & 0 \\ 0 & 0 & 0 & 0 & 0 & 0 & 0 & 0 & 0 & 0 \end{bmatrix},$$

and,

$$V = \begin{bmatrix} K_1 & 0 & 0 & 0 & 0 & -\alpha_{21} & 0 & 0 & 0 & 0 \\ -\sigma_1 & K_2 & 0 & 0 & 0 & 0 & -\alpha_{21} & 0 & 0 & 0 \\ 0 & -r\sigma_p & K_3 & 0 & 0 & 0 & 0 & -\alpha_{21} & 0 & 0 \\ 0 & -(1-r)\sigma_p & 0 & K_4 & 0 & 0 & 0 & 0 & -\alpha_{21} & 0 \\ 0 & 0 & -\phi_{1I} & 0 & K_5 & 0 & 0 & 0 & 0 & -\alpha_{21} \\ -\alpha_{12} & 0 & 0 & 0 & 0 & K_6 & 0 & 0 & 0 & 0 \\ 0 & -\alpha_{12} & 0 & 0 & 0 & 0 & K_7 & 0 & 0 & 0 \\ 0 & 0 & -\alpha_{12} & 0 & 0 & 0 & -q\sigma_p & K_8 & 0 & 0 \\ 0 & 0 & 0 & -\alpha_{12} & 0 & 0 & -(1-q)\sigma_p & 0 & K_9 & 0 \\ 0 & 0 & 0 & 0 & -\alpha_{12} & 0 & 0 & -\phi_{2I} & 0 & K_{10} \end{bmatrix},$$

where $K_1 = \alpha_{12} + \sigma_1 + \mu, K_2 = \alpha_{12} + \sigma_P + \mu, K_3 = \alpha_{12} + \phi_{1I} + \gamma_{1I} + \mu + \delta_{1I}, K_4 = \alpha_{12} + \gamma_{1A} + \mu, K_5 = \alpha_{12} + \gamma_{1H} + \mu + \delta_{1H}, K_6 = \alpha_{21} + \sigma_2 + \mu, K_7 = \alpha_{21} + \sigma_P + \mu, K_8 = \alpha_{21} + \phi_{2I} + \gamma_{2I} + \mu + \delta_{2I}, K_9 = \alpha_{21} + \gamma_{2A} + \mu$ and $K_{10} = \alpha_{21} + \gamma_{2H} + \mu + \delta_{2H}$.

For mathematical tractability, the computations will be carried out for the special case of the model $\{(2.1), (2.2)\}$ in the absence of the back-and-forth transitions between the no-mask and mask-user groups (i.e., the special case of the model with $\alpha_{12} = \alpha_{21} = 0$). Hence, from now on, we set $\alpha_{12} = \alpha_{21} = 0$. It follows that the *control reproduction number* of the model $\{(2.1), (2.2)\}$ (with $\alpha_{12} = \alpha_{21} = 0$), denoted by $\mathcal{R}_c$, is given by (where ρ is the spectral radius):

$$\mathcal{R}_c = \rho(FV^{-1}) = \max\{\mathcal{R}_{c_1}, \ \mathcal{R}_{c_2}\}, \tag{3.4}$$

where,

$$\mathcal{R}_{c_1} = (a_{11} + a_{22}) + \sqrt{(a_{22} - a_{11})^2 + 4\, a_{21} a_{12}}, \text{ and } \mathcal{R}_{c_2} = (a_{11} + a_{22}) - \sqrt{(a_{22} - a_{11})^2 + 4\, a_{21} a_{12}}, \tag{3.5}$$

with a_{11}, a_{12}, , a_{21} and a_{22} defined in Appendix II. The result below follows from Theorem 2 of [28].

Theorem 3.2. *The DFE ($\mathbb{E}_0$) of the special case of the model $\{(2.1), (2.2)\}$, with $\alpha_{12} = \alpha_{21} = 0$, is locally-asymptotically stable if $\mathcal{R}_c < 1$, and unstable If $\mathcal{R}_c > 1$.*

The threshold quantity $\mathcal{R}_c$ is the *control reproduction number* of the model $\{(2.1), (2.2)\}$. It measures the average number of new COVID-19 cases generated by a typical infectious individual introduced into a population where a certain fraction of the population is protected (*via* the use of interventions, such as face mask, social-distancing and/or vaccination). The epidemiological implication of Theorem 3.2 is that a small influx of COVID-19 cases will not generate an outbreak in the community if the control reproduction number ($\mathcal{R}_c$) is brought to, and maintained at a, value less than unity.

In the absence of public health interventions (i.e., in the absence of vaccination, face mask usage and social-distancing), the control reproduction number ($\mathcal{R}_c$) reduces to the *basic reproduction number* (denoted by $\mathcal{R}_0$), given by:

$$\mathcal{R}_0 = \mathcal{R}_c|_{c_s=\varepsilon_0=\varepsilon_i=\varepsilon_v=S^*_{1v}=S^*_{2v}=0} = \max\{\mathcal{R}_1, \ \mathcal{R}_2\}, \tag{3.6}$$

where,

$$\mathcal{R}_1 = (b_{11} + b_{22}) + \sqrt{(b_{22} - b_{11})^2 + 4\, b_{21} b_{12}}, \text{ and } \mathcal{R}_2 = (b_{11} + b_{22}) - \sqrt{(b_{22} - b_{11})^2 + 4\, b_{21} b_{12}}, \tag{3.7}$$

with b_{11}, b_{12}, b_{21} and b_{22} defined in Appendix II.

3.2 Vaccine-induced Herd Immunity Threshold

Herd immunity is a measure of the minimum percentage of the number of individuals in a community that is susceptible to a disease that need to be protected (i.e., become immune) so that the disease can be eliminated from the population. There are two main ways to achieve herd immunity, namely through acquisition of natural immunity (following natural recovery from infection with the disease) or by vaccination. Vaccination is the safest and fastest way to achieve herd immunity [30, 31]. For vaccine-preventable diseases, such as COVID-19, not every susceptible member of the community can be vaccinated, for numerous reasons (such as individuals with certain underlying medical conditions, infants, pregnant women, or those who opt out of being vaccinated for various reasons etc.) [7]. So, the question, in the context of vaccine-preventable diseases, is what is the minimum proportion of individuals that can be vaccinated we need to vaccinate in order to achieve herd immunity (so that those individuals that cannot be vaccinated will become protected owing to the community-wide herd-immunity). In this section, a condition for achieving vaccine-derived herd immunity in the U.S. will be derived.

It is convenient to define (where N_1^* and N_2^* represent the total size of the sub-population of Group 1 and Group 2 at disease-free equilibrium, respectively):

$$q_1 = (1-c_s)\left[\frac{S_{1u}^* + (1-\varepsilon_v)S_{1v}^*}{N_1^*}\right] \text{ and } q_2 = (1-c_s)\left[\frac{S_{2u}^* + (1-\varepsilon_v)S_{2v}^*}{N_2^*}\right]. \tag{3.8}$$

Using Equation (3.8), the expressions for a_{11}, a_{12}, a_{21} and a_{22} in Appendix II can be re-written as:

$$a_{11} = q_1 b_{11}, \;\; a_{12} = q_1(1-\varepsilon_0)b_{12}, \;\; a_{21} = q_2(1-\varepsilon_i)b_{21}, \;\; a_{22} = q_2(1-\varepsilon_i)(1-\varepsilon_0)b_{22}. \tag{3.9}$$

Furthermore, using (3.9) in (3.4) gives:

$$\mathcal{R}_c = [q_1 b_{11} + q_2(1-\varepsilon_i)(1-\varepsilon_0)b_{22}] + \sqrt{[q_2(1-\varepsilon_i)(1-\varepsilon_0)b_{22} - q_1 b_{11}]^2 + 4q_1 q_2 b_{12} b_{21}(1-\varepsilon_i)(1-\varepsilon_0)}. \tag{3.10}$$

Let $f_{1v} = S_{1v}^*/N_1^*$ and $f_{2v} = S_{2v}^*/N_2^*$ be the proportions of susceptible individuals in Groups 1 and 2, respectively, that have been vaccinated at the disease-free equilibrium ($\mathbb{E}_0$). Hence, (3.8) can be re-written (in terms of f_{1v} and f_{2v}) as:

$$q_1 = (1-c_s)(1-f_{1v}\varepsilon_v) \text{ and } q_2 = (1-c_s)(1-f_{2v}\varepsilon_v). \tag{3.11}$$

In order to compute the expression for the herd immunity threshold associated with the model $\{(2.1), (2.2)\}$, it is convenient to let $f_v = \max\{f_{1v}, \; f_{2v}\}$. Using this definition in Equation (3.10) gives:

$$\mathcal{R}_c = (1-c_s)(1-f_v\varepsilon_v)\left\{[b_{11} + (1-\varepsilon_i)(1-\varepsilon_0)b_{22}] + \sqrt{[(1-\varepsilon_i)(1-\varepsilon_0)b_{22} - b_{11}]^2 + 4b_{12}b_{21}(1-\varepsilon_i)(1-\varepsilon_0)}\right\}. \tag{3.12}$$

Setting $\mathcal{R}_c$, in Equation (3.12), to unity and solving for f_v gives the herd immunity threshold (denoted by f_v^c):

$$\begin{aligned} f_v &= \frac{1}{\epsilon_v}\left\{1 - \frac{1}{(1-c_s)[b_{11} + (1-\varepsilon_i)(1-\varepsilon_0)b_{22}] + \sqrt{[(1-\varepsilon_i)(1-\varepsilon_0)b_{22} - b_{11}]^2 + 4b_{12}b_{21}(1-\varepsilon_i)(1-\varepsilon_0)}}\right\} \\ &= f_v^c. \end{aligned} \tag{3.13}$$

It follows from (3.13) that $\mathcal{R}_c < (>) 1$ if $f_v > (<) f_v^c$. Further, $\mathcal{R}_c = 1$ whenever $f_v = f_v^c$. This result is summarized below:

Theorem 3.3. *Consider the special case of the model $\{(2.1), (2.2)\}$ with $\alpha_{12} = \alpha_{21} = 0$. Vaccine-induced herd immunity (i.e., COVID-19 elimination) can be achieved in the U.S., using an imperfect anti-COVID vaccine, if $f_v > f_v^c$ (i.e., if $\mathcal{R}_c < 1$). If $f_v < f_v^c$ (i.e., if $\mathcal{R}_c > 1$), then the vaccination program will fail to eliminate the COVID-19 pandemic in the U.S.*

The epidemiological implication of Theorem 3.3 is that the use of an imperfect anti-COVID vaccine can lead to the elimination of the COVID-19 pandemic in the U.S. if the sufficient number of individuals residing in the U.S. is vaccinated, such that $f_v > f_v^c$. The Vaccination program will fail to eliminate the pandemic if the vaccine coverage level is below the aforementioned herd immunity threshold (i.e., if $f_v < f_v^c$). Although vaccination, no matter the coverage level, is always useful (i.e., vaccination will always reduce the associated reproduction number, $\mathcal{R}_c$, thereby reducing disease burden, even if the program is unable to bring the reproduction number to a value less than unity), elimination can only be achieved if the herd immunity threshold is reached (i.e., disease elimination is only feasible if the associated reproduction number of the model is reduced to, and maintained at, a value less than unity). The pandemic will persist in the U.S. if $\mathcal{R}_c > 1$. Figure 3 depicts the cumulative mortality of COVID-19 in the U.S. for various steady-state vaccination coverage levels (denoted by f_v). This figure shows a decrease in cumulative mortality with increasing vaccination coverage. In particular, a marked decrease in cumulative mortality is recorded when herd immunity (i.e., $f_v > f_v^c$) is reached in the population.

Furthermore, Figure 4 depicts a contour plot of the control reproduction number ($\mathcal{R}_c$) of the model, as a function of vaccination efficacy (ε_v) and coverage (f_v). This figure shows that the reproduction number decreases with increasing values of vaccination efficacy and coverage. For instance, this figure shows that, with the baseline level of social-distancing and face-mask usage in the U.S., although the AstraZeneca vaccine (with estimated efficacy of 75%) can significantly reduces the reproduction number (from $\mathcal{R}_c \approx 4.5$ to about $\mathcal{R}_c \approx 1.5$ (hence, greatly reduce disease burden), it is unable to lead to the elimination of the disease even if every member of the U.S. population is vaccinated. However, such elimination is feasible using the AstraZeneca vaccine if the coverage level of social-distancing is increased from the baseline (Table 2). For instance, if 60% of the U.S. population observe social-distancing in public, the AstraZeneca vaccine can lead to COVID-19 elimination in the U.S. if about 89% of the populace is vaccinated. The vaccination coverage needed to achieve elimination (using AstraZeneca vaccine) decreases to a mere 35% if 80% of Americans will socially-distant in public (Table 2). If, on the other hand, either the Moderna or Pfizer vaccine (with estimated efficacy of about 95%) is used, Figure 4 shows that, based on the current baseline level of social-distancing coverage, vaccinating about 83% of the population will lead to the elimination of the pandemic in the U.S. The vaccine coverage level needed to eliminate the pandemic (using either of the Pfizer or Moderna vaccine) dramatically decreases to 26% if 80% social-distancing coverage can be reached (Table 2).

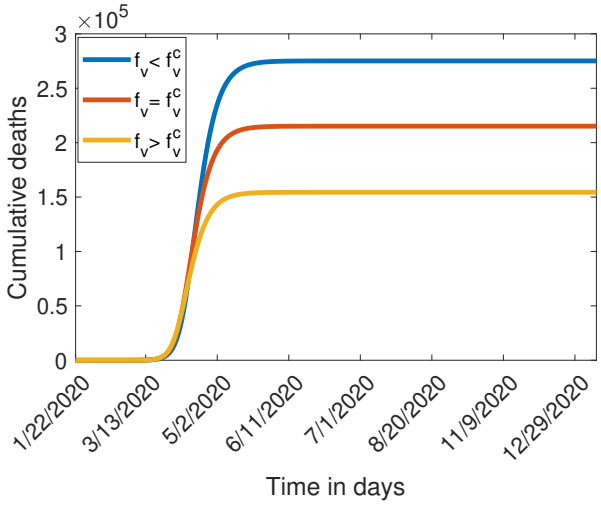

Figure 3: Simulations of the special case of the model $\{(2.1), (2.2)\}$, with $\alpha_{12} = \alpha_{21} = 0$, showing the cumulative COVID-19 mortality in the U.S., as a function of time. (a) $f_v < f_v^c\,(r = 0.5)$ (b) $f_v = f_v^c\,(r = 0.7)$ (c) $f_v > f_v^c\,(r = 0.9)$. Other parameter values used in the simulations are as given in Table 1, with $\alpha_{12} = \alpha_{21} = 0$.

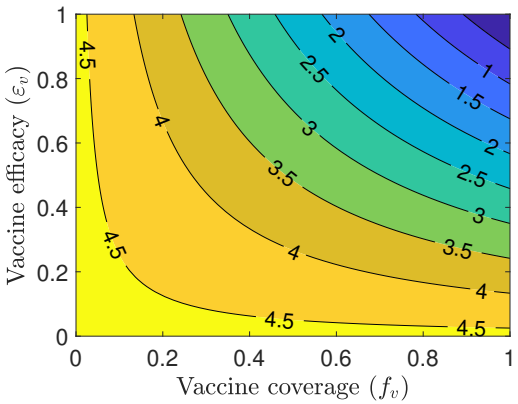

Figure 4: Contour plot of the control reproduction number ($\mathcal{R}_c$) of the model $\{(2.1), (2.2)\}$, with $\alpha_{12} = \alpha_{21} = 0$, as a function of vaccine coverage (f_v) and vaccine efficacy (ε_v), for the US. Parameter values used are as given in Table 1, with $\alpha_{12} = \alpha_{21} = 0$.

Table 2: Herd immunity threshold (f_v) for the U.S. for various levels of social-distancing coverage (c_s). Parameter values used are as given in Table 1, with $\alpha_{12} = \alpha_{21} = 0$.

	Herd threshold	**Herd threshold**	**Herd threshold**	**Herd threshold**
Vaccine type (efficacy)	$c_s = 30\%$	$c_s = 40\%$	$c_s = 60\%$	$c_s = 80\%$
AstraZeneca ($\varepsilon_v = 70\%$)	$f_v = 112\%$	$f_v = 107\%$	$f_v = 89.1\%$	$f_v = 35.3\%$
Pfizer & Moderna ($\varepsilon_v = 95\%$)	$f_v = 82.5\%$	$f_v = 78.9\%$	$f_v = 65.7\%$	$f_v = 26\%$

4 Numerical Simulations: Assessment of Control Strategies

The model $\{(2.1), (2.2)\}$ will now be simulated to assess the population-level impact of the various intervention strategies described in this study. In particular, the singular and combined impact of social-distancing, face mask usage and the three candidate vaccines (by AstraZeneca, Moderna and Pfizer) on curtailing (or eliminating) the burden of the COVID-19 pandemic in the U.S. will be assessed. Unless otherwise stated, the simulations will be carried out using the estimated and baseline values of the parameters of the model tabulated in Table 1. Further, the baseline initial condition for the face mask use group (assumed to be 1%) will be used.

4.1 Assessing the impact of mask-use

The model (2.1)-(2.2) is simulated to assess the community-wide impact of using face-masks alone on the pandemic in the United States. Specifically, we simulate the model using the baseline values of the parameters in Table 1 and various initial values of the number of individuals who habitually wear face masks in public, right from the very beginning of the pandemic (denoted by $N_2(0)$). It should be noted that the parameters associated with other interventions (e.g., vaccination-related and social-distancing-related parameters) are kept at their baseline values given in Table 1. The simulation results obtained, depicted in Figure 5, generally show that the early adoption of face masks measures play a vital role in curtailing the COVID-related mortality in the U.S., particularly for the case when mask-wearers do not opt to give up mask wearing (i.e., when $\alpha_{21} \neq 0$). For the case where the parameters associated with the back-and-forth transitions between the masking and non-masking groups (i.e., α_{12} and α_{21}) are maintained at their baseline values (given in Table 1), this figure shows that the size of the initial number of individuals who wear face masks, right from the beginning of the pandemic, has only marginal impact on the cumulative COVID-related mortality in the U.S., as measured in relation to the cumulative mortality recorded when the initial population of mask wearers is at the 1% baseline level (Figure 5 (a)). On the other hand, for the case when mask-wearers remain mask-wearers since the very beginning of the pandemic (i.e., $\alpha_{21} = 0$), while

non-maskers in Group 1 can change their behavior and become mask-wearers (i.e., $\alpha_{12} \neq 0$), the initial number of individuals who adopt masking from the beginning of the pandemic has a more pronounced effect on the cumulative mortality (Figure 5 (b)), in relation to the baseline. In particular, if 25% of the U.S. population adopt mask-wearing right from the beginning of the pandemic (and remain mask-wearers), up to 6% of COVID-related mortality can be averted, in relation to the 1% baseline mask-wearing at the beginning of the pandemic (green curve, Figure 5 (b)). Further, the reduction in cumulative mortality rises to 11% (in relation to the baseline) could be achieved if half of Americans opted to wear face masks since the very beginning of the pandemic (blue curve, Figure 5 (b)). For the case when no back-and-forth transitions between the two (mask-wearing and non-mask-wearing) groups is allowed (i.e., when $\alpha_{12} = \alpha_{21} = 0$), our simulations show a far more dramatic effect of face mask usage in reducing COVID-19 mortality (Figure 5 (c)). In particular, we showed that up to 24% cumulative mortality can be averted, in comparison to the baseline (magenta curve), if 25% of the U.S. population adopted mask-wearing mandate right from the beginning of the pandemic (green curve, Figure 5 (c)). Furthermore, 49% of the cumulative mortality could have been prevented if 50% of the U.S. population were wearing face masks since the beginning of the pandemic (blue curve, Figure 5 (c)).

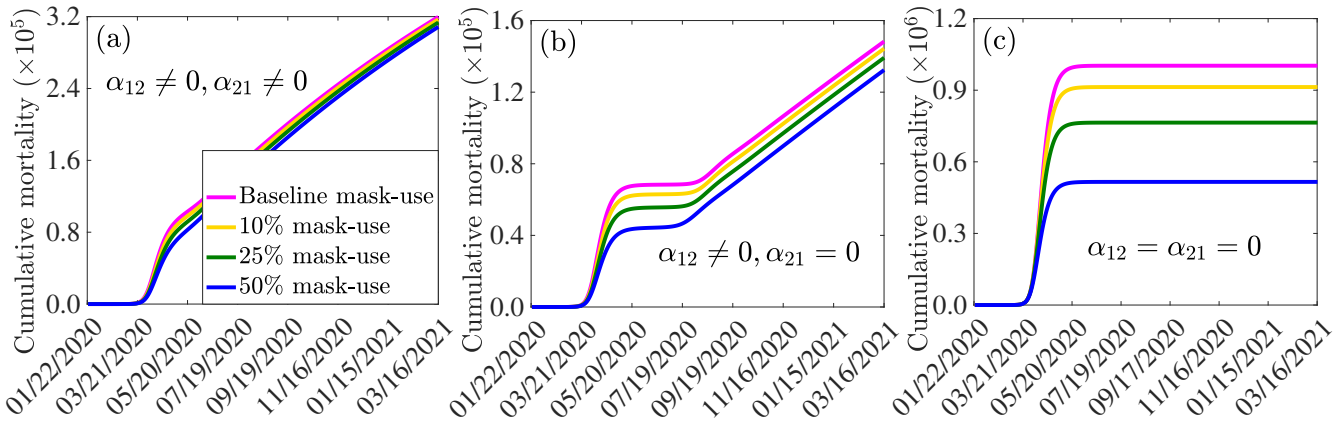

Figure 5: Assessment of the singular impact of face mask usage on COVID-19 pandemic in the U.S. Simulations of the model (2.1)-(2.2), showing cumulative COVID-induced mortality, as a function of time, for (a) face mask transition parameters (α_{12} and α_{21}) maintained at their baseline values, (b) mask-wearers strictly adhere to wearing masks ($\alpha_{21} = 0$) and non-mask-wearers transit to mask wearing at their baseline rate ($\alpha_{12} \neq 0$), (c) non-mask wearers and mask-wearers do not change their behavior (i.e., $\alpha_{12} = \alpha_{21} = 0$). Mask use change is implemented in terms of changes in the initial population of individuals who wear face-masks (i.e., in terms of changes in the initial total population size in Group 2, $N_2(0)$). Parameter values used in the simulations are as given by the baseline values in Table 1, with different values of α_{12} and α_{21}.

4.2 Assessing the impact of social-distancing

In this section, we carry out numerical simulations to assess whether social-distancing alone (implemented right from the very beginning of the pandemic) might be sufficient to contain the COVID-19 pandemic in the U.S. To achieve this objective, the model $\{(2.1), (2.2)\}$ is simulated using the parameters in Table 1 with various levels of the social-distancing compliance parameter (c_s) and all other control-related parameters (e.g., initial face mask coverage and efficacy, vaccination rate and efficacy etc.) are maintained at their baseline values.

The simulation results obtained, depicted in Figure 6, show that the cumulative mortality (Figure 6 (a)) and daily mortality (Figure 6 (b)) decrease with increasing social-distancing compliance. In the absence of social-distancing (i.e., $c_s = 0$), the simulations show that the U.S. could record up to $422,013$ cumulative deaths by September 12, 2021 (Figure 6 (a), red curve). For this (social-distancing-free) scenario, the U.S. will record a peak daily mortality of about $6,585$ deaths on March 21, 2020 (Figure 6 (b), red curve). It is further shown that, if 30% of the U.S. population will be observing social-distancing in public, up to 24% reduction can be recorded in the cumulative mortality, in relation to the cumulative mortality recording for the social-distancing-

free scenario (Figure 6 (a), magenta curve). Similarly, up to 51% reduction can be achieved in daily mortality (Figure 6 (b), magenta curve), and the pandemic would have peaked a month later (in April 2020; the daily mortality at this peak would have been $3,247$). Further dramatic reduction in COVID-19 mortality is recorded as social-distancing compliance is further increased. For instance, if 60% of the U.S. population adhere to the social-distancing measures, about 62% of the cumulative deaths recorded (for the case with $c_s = 0$) would have been averted (Figure 6 (a), green curve). For this scenario, 87% of the daily deaths would have been prevented and the pandemic would have peaked in June 2020 (the daily mortality at this peak would have been 864). Finally, if 75% of the U.S. population complied with the social-distancing measures, right from the beginning of the pandemic, the COVID-19 pandemic would have failed to generate a major outbreak in the U.S. (Figure 6, blue curves). In particular, the cumulative mortality for the entire U.S. by September 21, 2021 will be about $20,000$. Thus, in summary, the simulations in Figure 6 show that COVID-19 could have been effectively suppressed in the U.S. using social-distancing at moderate to high compliance levels.

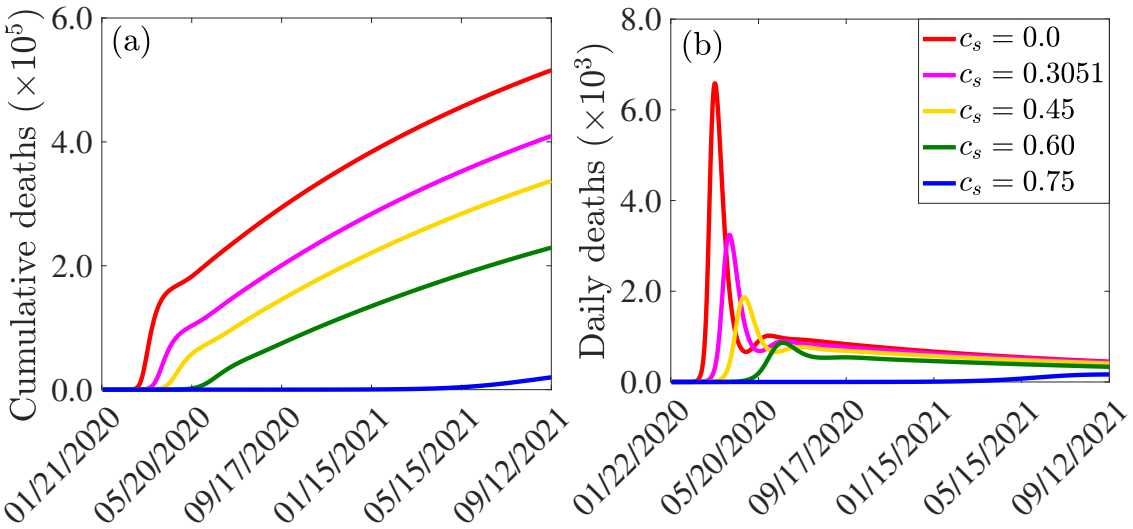

Figure 6: Assessment of the singular impact of social-distancing on COVID-19 pandemic in the U.S. Simulations of the model (2.1)-(2.2) showing (a) cumulative mortality, as a function of time; (b) daily mortality, as a function of time, for various compliance levels of the social-distancing parameter (c_s). Initial conditions used are: $(S_1^0, E_1^0, P_1^0, I_1^0, A_1^0, H_1^0, R_1^0, S_2^0, E_2^0, P_2^0, I_2^0, A_2^0, H_2^0, R_2^0) = (0.99 \times 336218660 - 1, 0, 0, 1, 0, 0, 0, 0.01 \times 336218660, 0, 0, 0, 0, 0, 0, 0)$. Parameter values used in the simulations are as given by the baseline values in Table 1.

4.3 Assessment of combined impact of vaccination and social-distancing

The model (2.1)-(2.2) will now be simulated to assess the community-wide impact of the combined vaccination and social-distancing interventions. Although the vaccines are expected to be available by the end of the year 2020 or early in 2021, we assume that there will be some time lag before the vaccines are made widely available to the general public. This is because the vaccines will initially be targeted to the people most at risk (notably the frontline healthcare workers, nursing home residents and staff, essential workers, people with underlying conditions etc.) before being made available to the general. For simulation purposes, we assume that the vaccines will be available to the general public by March 15, 2021.

We consider the three vaccines currently on the verge of being approved by the FDA for use in humans, namely the AstraZeneca vaccine (with estimated efficacy of 70%) and the Moderna and Pfizer vaccines (each with estimated efficacy of about 95%). Simulations are carried out using the baseline parameter values in Table 1, with various values of the vaccination coverage parameter (ξ_v). For these simulations, parameters and initial conditions related to the other intervention (face mask usage) are maintained at their baseline values. Since the Moderna and Pfizer vaccines have essentially the same estimated efficacy ($\approx 95\%$), we group them together in the simulations.

The simulation results obtained for the AstraZeneca vaccine, depicted in Figures 7 (a)-(c)), show that, in the absence of vaccination (and with social-distancing at baseline compliance level), approximately $1,388$ will be recorded on August 31, 2021 (red curves of Figures 7 (a)-(c)). Furthermore, this figure shows a marked reduction in daily mortality with increasing vaccination coverage (ξ_v). This reduction further increases if vaccination is combined with social-distancing (particularly with high enough compliance). For instance, with social-distancing compliance maintained at its baseline value ($c_s = 0.3015$), vaccinating at a rate of 0.00074 *per* day (which roughly translates to vaccinating $250,000$ people every day) resulted in a reduction of the projected daily mortality on August 31, 2021 by 14% (in comparison to the case when no vaccination is used; magenta curve in Figure 7 (a)). In fact, up to 78% of the projected daily mortality for August 31, 2021 could be averted if, for this vaccination rate, 60% social-distancing compliance is attained (magenta curve in Figure 7 (c)). If the vaccination rate is further increased to, for instance, $\xi_v = 0.0015$ *per* day (corresponding to vaccinating about $500,000$ people every day), our simulations show a reduction of 26% in the projected daily mortality on August 31, 2021 if social-distancing is maintained at its baseline level (gold curve, Figure 7 (a)). This reduction increases to 85% if the vaccination program is supplemented with social-distancing with 60% compliance (gold curve, Figures 7 (c)). If 1 million people are vaccinated *per* day (i.e., $\xi_v = 0.003$) *per* day, our simulations show that the use of AstraZeneca vaccine could lead to up to 46% reduction in the projected daily mortality on August 31, 2021 if the vaccination program is combined with social-distancing at baseline compliance level. Further reductions in the projected daily mortality are recorded when either the Moderna or Pfizer vaccine (with moderate to high vaccination coverage) is used (Figures 7 (d)-(f)), particularly if combined with social-distancing with high compliance (blue curves in Figures 7 (d)-(f)). These results are summarized in Table 3.

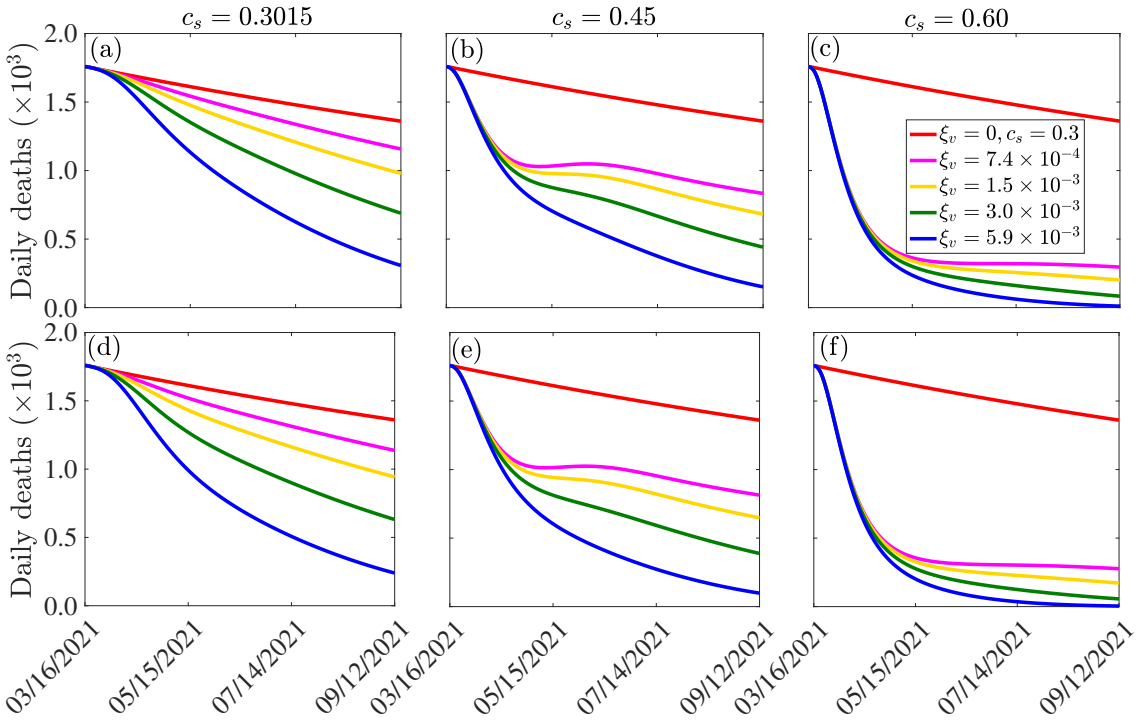

Figure 7: Assessment of the combined impact of vaccination and social-distancing on daily mortality. Simulations of the model (2.1)-(2.2), depicting daily mortality as a function of time, for various vaccine types and social-distancing compliance (c_s). (a)-(c): AstraZeneca vaccine. (d)-(f): Pfizer or Moderna vaccine. The vaccination rates $\xi_v = 7.4 \times 10^{-4}, 1.5 \times 10^{-3}, 3.0 \times 10^{-3}, 5.9 \times 10^{-3}$ correspond, respectively, to vaccinating approximately $2.5 \times 10^5, 5.0 \times 10^5, 1.0 \times 10^6, 2.0 \times 10^6$ people *per* day. Other parameter values of the model are as presented in Table 1.

Table 3: Percentage reduction in projected daily mortality on August 31, 2021, in relation to the daily mortality in the absence of vaccination (1,383 COVID-19 deaths on August 31, 2021), for different types of COVID-19 vaccines: AstraZeneca vaccine (efficacy $\varepsilon_v = 0.7$); Pfizer and/or Moderna vaccine (efficacy $\varepsilon_v = 0.95$), and various compliance levels of social-distancing (c_s) and number of individuals vaccinated *per* day.

Number of people vaccinated *per* day	**Reduction with** $c_s = 0.3051$		**Reduction with** $c_s = 0.45$		**Reduction with** $c_s = 0.60$	
	$\varepsilon_v = 70\%$	$\varepsilon_v = 95\%$	$\varepsilon_v = 70\%$	$\varepsilon_v = 95\%$	$\varepsilon_v = 70\%$	$\varepsilon_v = 95\%$
250,000	14%	15%	38%	39%	78%	79%
500,000	26%	29%	48%	51%	85%	87%
1,000,000	46%	51%	65%	69%	93%	95%
2,000,000	74%	80%	87%	91%	98.8%	99.5%

4.4 Impact of vaccination and social-distancing on time to pandemic elimination

The model (2.1)-(2.2) will now be simulated to assess the community-wide impact of the combined vaccination and social-distancing interventions on the expected time the implementation of these interventions will take to result in the elimination of the pandemic in the U.S. (i.e., time needed for the number of new COVID-19 cases to be essentially zero). As in Section 4.3, we consider the three candidate vaccines (the AstraZeneca, Moderna and the Pfizer vaccines). The model is simulated to generate a time series of new daily COVID-19 cases in the U.S., for various vaccination coverage and social-distancing compliance levels. The results obtained, for the AstraZeneca vaccine, depicted in Figures 8 (a)-(c), show a marked decrease in the time-to-elimination with increasing vaccination coverage and social-distancing compliance. In particular, vaccinating 250,000 people *per* day, with the AstraZeneca vaccine, will result in COVID-19 elimination in the U.S. by late October of 2025, if the social-distancing compliance is kept at its current baseline level of 30.51% (red curve of Figure 8 (a)). For this scenario, the elimination will be reached in early October 2025 using either the Moderna or the Pfizer vaccine. If the vaccination rate is further increases, such as vaccinating 1 million people every day, COVID-19 elimination is achieved much sooner. For instance, for this scenario (i.e., $\xi_v = 0.003$ *per* day), the pandemic can be eliminated, using the AstraZeneca vaccine, by mid July of 2022 if the vaccination program is combined with social-distancing at 60% compliance (green curve of Figure 8 (c)). Here, too, using the Moderna or the Pfizer vaccine can lead to the elimination of the pandemic a little sooner (by mid June 2022) if social-distancing is maintained at 60% (green curve, Figure 8 (f)). A summary of time-to-elimination for the aforementioned, and other, scenarios is given in Table 4. In conclusions, these simulations show that any of the three candidate vaccines considered in this study will lead to the elimination of the U.S. The time-to-elimination depends on the vaccination rate and the compliance level of social-distancing. The pandemic can be eliminated by as early as June of 2022 if moderate to high vaccination rate (e.g., 1 million people are vaccinated *per* day) and social-distancing compliance (e.g., $c_s = 0.6$) are attained and maintained.

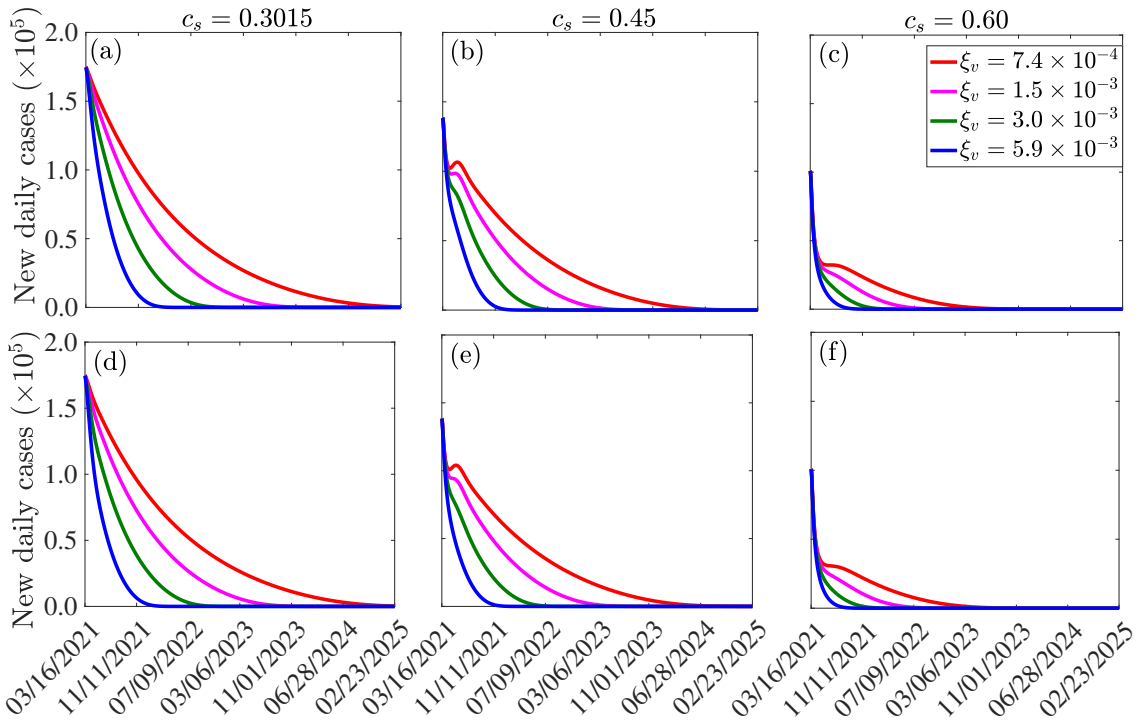

Figure 8: Effect of vaccination and social-distancing on time-to-elimination. Simulations of the model (2.1)-(2.2), depicting the impact of three candidate vaccines against COVID-19 (the AstraZeneca vaccine, and the Pfizer or Moderna vaccine) and social-distancing, on time-to-elimination of the pandemic in the U.S. (a)-(c): AstraZeneca vaccine. (d)-(f): Moderna or Pfizer vaccine. The social-distancing compliance is $c_s = 0.3051$ for (a) and (d), $c_s = 0.45$ for (b) and (e), and $c_s = 0.60$ for (e) and (f). The vaccination rates $\xi_v = 7.4 \times 10^{-4}, 1.5 \times 10^{-3}, 3.0 \times 10^{-3}, 5.9 \times 10^{-3}$ correspond, respectively, to vaccinating approximately $2.5 \times 10^5, 5.0 \times 10^5, 1.0 \times 10^6, 2.0 \times 10^6$ people *per* day. The values of the other parameters of the model used in the simulation are as given in Table 1.

Table 4: Time to eliminate the COVID-19 pandemic in the U.S., for various values of the vaccination rate (ξ_v) using the three candidate vaccines (AstraZeneca vaccine with efficacy $\varepsilon_v = 70\%$; the Moderna or Pfizer vaccine with efficacy $\varepsilon_v = 95\%$) and various levels of social-distancing compliance (c_s). Parameter values used are as given in Table 1.

Number of people vaccinated *per* day	**Reduction with** $c_s = 0.3051$		**Reduction with** $c_s = 0.45$		**Reduction with** $c_s = 0.60$	
	$\varepsilon_v = 70\%$	$\varepsilon_v = 95\%$	$\varepsilon_v = 70\%$	$\varepsilon_v = 95\%$	$\varepsilon_v = 70\%$	$\varepsilon_v = 95\%$
250,000	10/26/2025	10/09/2025	07/08/2025	07/15/2025	07/03/2024	06/06/2024
500,000	05/19/2024	05/14/2024	01/10/2024	12/26/2023	04/25/2023	04/02/2023
1,000,000	03/26/2023	03/06/2023	12/31/2022	12/11/2022	07/14/2022	06/18/2022
2,000,000	06/24/2022	06/09/2022	04/24/2022	04/05/2022	01/14/2022	12/21/2021

5 Discussion and Conclusions

Since its emergence late in December of 2019, the novel Coronavirus pandemic continues to inflict devastating public health and economic burden across the world. As of December 5, 2020, the pandemic accounted for over 67 million confirmed cases and over 1.5 million deaths globally. Although control efforts against the pandemic have focused on the use of non-pharmaceutical interventions, such as social-distancing, face mask usage, quarantine, self-isolation, contact-tracing, community lockdowns, etc., a number of highly promising (safe and highly-efficacious)

anti-COVID vaccines are currently on the verge of being approved by the Food and Drug Administration (FDA) for use in humans. In particular, two vaccine manufacturers, Moderna Inc. and Pfizer Inc., filed for Emergency Use Authorization with the FDA in November 2020 (each of the two vaccines has estimated protective efficacy of about 95%). Furthermore, AstraZeneca vaccine, developed by the pharmaceutical giant, AstraZeneca, and University of Oxford, UK, is undergoing Phase III of clinical trials with very promising results (estimated efficacy of 70%). Mathematics (modeling, analysis and data analytics) has historically been used to provide robust insight into the transmission dynamics and control of infectious diseases, dating back to the pioneering works of the likes of Daniel Bernoulli in the 1760s (on smallpox immunization), Sir Ronald Ross and George Macdonald between the 1920s and 1950s (on malaria modeling) and the compartmental modeling framework developed by Kermack and McKendrick in the 1920s [32–34]. In this study we have used mathematical modeling approaches, coupled with rigorous analysis, to assess the potential population-level impact of the wide scale deployment of any (or combination of) the aforementioned candidate vaccines in curtailing the burden of the COVID-19 pandemic in the U.S. We have also assessed the impact of other non-pharmaceutical interventions, such as face mask and social-distancing, implemented singly or in combination with any of the three vaccines, on the dynamics and control of the pandemic in the U.S.

We developed a novel mathematical model, which stratifies the total population into two subgroups of individuals who habitually wear face masks in public and those who do not. The resulting two group COVID-19 vaccination model, which takes the form of a deterministic system of nonlinear ordinary differential equations, was initially fitted using observed cumulative COVID-induced mortality data for the U.S. The model allowed for the assessment of social-distancing measures on combating the spread of the pandemic. The model was then rigorously analysed to gain insight into its dynamical features. In particular, we showed that the disease-free equilibrium of the model is locally-asymptotically stable whenever a certain epidemiological threshold, known as the *control reproduction number* (denoted by $\mathcal{R}_c$), is less than unity. The implication of this result is that (for the case when $\mathcal{R}_c < 1$), a small influx of COVID-infected individuals will not generate an outbreak in the community.

The expression for the reproduction number ($\mathcal{R}_c$) was used to compute the nationwide vaccine-induced *herd immunity* threshold. The herd immunity threshold represents the minimum proportion of the U.S. population that needs to be vaccinated to ensure elimination of the pandemic. Simulations of our model shows, for the current baseline level of social-distancing in the U.S. (at 30%), herd immunity cannot be achieved in the U.S. using the AstraZeneca vaccine. However, achieving such herd immunity threshold is feasible using either the Moderna or the Pfizer vaccine if at least 83% of the U.S. residents are vaccinated. Our simulations further showed that the level of herd immunity needed to eliminate the pandemic decreases, for each of the three vaccines, with increasing social-distancing compliance. In particular, if 80% of American residents adhere to social-distancing, vaccinating only 35% and 26% with the AstraZeneca or Moderna/Pfizer vaccine, respectively, will generate the desired herd immunity. In other words, this study shows that the prospect of achieving vaccine-derived herd immunity, using any of the three candidate vaccines, is very promising, particularly if the vaccination program is complemented with social-distancing measures with moderate to high compliance levels.

This study also shows that the use of any of the three vaccines (i.e., the AstraZeneca, Pfizer, or Moderna vaccine) will dramatically reduce the burden of the COVID-19 pandemic in the U.S. (as measured in terms of cumulative or daily COVID-induced mortality). The level of reduction achieved increases with increasing daily vaccination coverage. Furthermore, the effectiveness of the vaccination program (using any of the three candidate vaccines), to reduce COVID-19 burden, is significantly enhanced if the vaccination program is complemented with other interventions, such as social-distancing (at moderate to high compliance levels). Our study further highlights the fact that early implementation of masks adoption (i.e., face mask adoption from the very beginning of the pandemic) plays a crucial role in effectively combating the burden of the COVID-19 pandemic (as measured in terms of reduction in cumulative COVID-related mortality) in the U.S. It was further shown that the level of such reduction is very sensitive to the rate at which mask-wearers opt to abandon mask-wearing (i.e., reverting to the group of non-mask wearers). In other words, our study emphasize the fact that early implementation or adoption of mask mandate, together with (strict) compliance to this mandate, plays a major role in effectively curtailing, or halting, the COVID-19 pandemic in the U.S.

We further showed that the time-to-elimination of COVID-19 in the U.S., using a vaccine (and a non-pharmaceutical

intervention), depends on the vaccination rate (i.e., number of people vaccinated everyday) and the level of compliance of social-distancing measures in the country. Specifically, our study shows that the COVID-19 pandemic can be eliminated in the U.S. by early June of 2022 if moderate to high vaccination rate (e.g., 1 million people vaccinated *per* day) and social-distancing compliance (e.g., 60% social-distancing compliance) are achieved and maintained. It should, however, be mentioned that the time-to-elimination is sensitive to the level of community transmission of COVID-19 in the population (it is also sensitive to the effectiveness and coverage (compliance) levels of the other (non-pharmaceutical) interventions, particularly face mask usage and social-distancing compliance, implemented in the community). Specifically, our study was carried out during the months of November and December of 2020, when the United States was experiencing a devastating third wave of the COVID-19 pandemic (recording an average of $200,000$ confirmed cases *per* day, together with record numbers of hospitalizations and COVID-induced mortality). This explains the somewhat *longer* estimated time-to-elimination of the pandemic, using any of the three vaccines, for the case where social-distancing compliance is low. The estimate for the time-to-elimination (using any of the three vaccines) will be shorter if the community transmission is significantly reduced (as will be vividly evident from the reduced values of the transmission- and mortality-related parameters of the re-calibrated version of our model).

From the derivation of our model, there is clearly an endemic disease equilibrium whose value we have not explicitly calculated, and whose existence and stability will signal the long term persistence of the disease in the population. However, since our analysis was geared towards eradication of the disease, the herd immunity thresholds determined here, that hold when the control reproduction number is less than unity, also serve as condition for the non-existence of the endemic equilibrium state in the absence of the phenomenon of backward bifurcation. These, and other aspects such as long term dynamics that have not been fully examined in the current analysis are aspects for further studies.

Acknowledgments

One of the authors (ABG) acknowledge the support, in part, of the Simons Foundation (Award #585022) and the National Science Foundation (Award #1917512). CNN acknowledges the support of the Simons Foundation (Award #627346). GAN acknowledge the grants and support of the Cameroon Ministry of Higher Education, through the initiative for the modernisation of research in Higher Education. All authors wish to express their deepest sympathy to the families of the victims of the SARS-CoV-2, and extend profound appreciation to the frontline healthcare workers for their heroic effort and sacrifices to save the lives of others.

Table 5: Description of the state variables of the model $\{(2.1), (2.2)\}$.

State variable	**Description**
S_{1u}	Population of non-vaccinated susceptible individuals who do not habitually wear face masks
S_{2u}	Population of non-vaccinated susceptible individuals who habitually face masks
S_{1v}	Population of vaccinated susceptible individuals who do not habitually wear face masks
S_{2v}	Population of vaccinated susceptible individuals who habitually wear face masks
E_1	Population of exposed (newly-infected) individuals who do not habitually wear face masks
E_2	Population of exposed (newly-infected) individuals who habitually wear face masks
P_1	Population of pre-symptomatic infectious individuals who do not habitually wear face masks
P_2	Population of pre-symptomatic infectious individuals who habitually wear face masks
I_1	Population of symptomatically-infectious individuals who do not habitually wear face masks
I_2	Population of symptomatically-infectious individuals who habitually wear face masks
A_1	Population of asymptomatically-infectious individuals who do not habitually wear face masks
A_2	Population of asymptomatically-infectious individuals who habitually wear face masks
H_1	Population of hospitalized individuals who do not habitually wear face masks
H_2	Population of hospitalized individuals who habitually wear face masks
R_1	Population of recovered individuals who do not habitually wear face masks
R_2	Population of recovered individuals who habitually wear face masks

Table 6: Description of the parameters of the model $\{(2.1), (2.2)\}$.

Parameters	**Description**
Π	Recruitment (birth or immigration) rate into the population
μ	Natural mortality rate
$\beta_{P1}(\beta_{P2})$	Effective contact rate for pre-symptomatic individuals who do not wear (wear) face masks
$\beta_{I1}(\beta_{I2})$	Effective contact rate for infectious symptomatic individuals who do not wear (wear) face masks
$\beta_{A1}(\beta_{A2})$	Effective contact rate for symptomatically-infectious individuals who do not wear (wear) face masks
$\beta_{H1}(\beta_{H2})$	Effective contact rate for hospitalized individuals who do not wear (wear) face masks
$0 < \epsilon_0 < 1$	Outward protective efficacy of face masks
$0 < \epsilon_i < 1$	Inward protective efficacy of face masks
ω_v	Vaccine waning rate
α_{12}	Rate at which non-habitual face masks wearers choose to become habitual wearers
α_{21}	Rate at which habitual face masks wearers choose to become non-habitual wearers
ξ_v	*Per capita* vaccination rate
$0 < \varepsilon_v < 1$	Protective efficacy of the vaccine
$\sigma_1(\sigma_2)$	Rate at which exposed individuals who do not wear (wear) face masks progress to the corresponding pre-symptomatic infectious stage
σ_P	Rate at which pre-symptomatic infectious individuals progress to symptomatically-infectious or asymptomatically-infectious stage
$r(q)$	Proportion of pre-symptomatic infectious individuals who do not wear (wear) face masks that become symptomatically-infectious
$\phi_{1I}(\phi_{2I})$	Hospitalization rate for symptomatically-infectious individuals who do not wear (wear) face masks
$\gamma_{1A}(\gamma_{2A})$	Recovery rate for asymptomatically-infectious individuals who do not wear (wear) face masks
$\gamma_{1I}(\gamma_{2I})$	Recovery rate for symptomatically-infectious individuals who do not wear (wear) face masks
$\gamma_{1H}(\gamma_{2H})$	Recovery rate for hospitalized individuals who do not wear (wear) face masks
$\delta_{1I}(\delta_{2I})$	Disease-induced mortality rate for symptomatically-infectious individuals who do not wear (wear) face masks
$\delta_{1H}(\delta_{2H})$	Disease-induced mortality rate for hospitalized individuals who do not wear (wear) face masks

Appendix I: Entries of the Non-negative Matrix F

$$f_1 = (1-c_s)\beta_{P_1}\left[\frac{S^*_{1u}+(1-\epsilon_v)S^*_{1v}}{N^*_1}\right], f_2 = (1-c_s)\beta_{I_1}\left[\frac{S^*_{1u}+(1-\epsilon_v)S^*_{1v}}{N^*_1}\right], f_3 = (1-c_s)\beta_{A_1}\left[\frac{S^*_{1u}+(1-\epsilon_v)S^*_{1v}}{N^*_1}\right],$$

$$f_4 = (1-c_s)\beta_{H_1}\left[\frac{S^*_{1u}+(1-\epsilon_v)S^*_{1v}}{N^*_1}\right], f_5 = (1-c_s)(1-\epsilon_0)\beta_{P_2}\left[\frac{S^*_{1u}+(1-\epsilon_v)S^*_{1v}}{N^*_1}\right],$$

$$f_6 = (1-c_s)(1-\epsilon_0)\beta_{I_2}\left[\frac{S^*_{1u}+(1-\epsilon_v)S^*_{1v}}{N^*_1}\right], f_7 = (1-c_s)(1-\epsilon_0)\beta_{A_2}\left[\frac{S^*_{1u}+(1-\epsilon_v)S^*_{1v}}{N^*_1}\right],$$

$$f_8 = (1-c_s)(1-\epsilon_0)\beta_{H_2}\left[\frac{S^*_{1u}+(1-\epsilon_v)S^*_{1v}}{N^*_2}\right], g_1 = (1-c_s)(1-\epsilon_i)\beta_{P_1}\left[\frac{S^*_{2u}+(1-\epsilon_v)S^*_{2v}}{N^*_2}\right],$$

$$g_2 = (1-c_s)(1-\epsilon_i)\beta_{I_1}\left[\frac{S^*_{2u}+(1-\epsilon_v)S^*_{2v}}{N^*_2}\right], g_3 = (1-c_s)(1-\epsilon_i)\beta_{A_1}\left[\frac{S^*_{2u}+(1-\epsilon_v)S^*_{2v}}{N^*_2}\right],$$

$$g_4 = (1-c_s)(1-\epsilon_i)\beta_{H_1}\left[\frac{S^*_{2u}+(1-\epsilon_v)S^*_{2v}}{N^*_2}\right], g_5 = (1-c_s)(1-\epsilon_i)(1-\epsilon_0)\beta_{P_2}\left[\frac{S^*_{2u}+(1-\epsilon_v)S^*_{2v}}{N^*_2}\right],$$

$$g_6 = (1-c_s)(1-\epsilon_i)(1-\epsilon_0)\beta_{I_2}\left[\frac{S^*_{2u}+(1-\epsilon_v)S^*_{2v}}{N^*_2}\right], g_7 = (1-\epsilon_i)(1-\epsilon_0)\beta_{A_2}\left[\frac{S^*_{2u}+(1-\epsilon_v)S^*_{2v}}{N^*_2}\right],$$

$$g_8 = (1-\epsilon_i)(1-\epsilon_0)\beta_{H_2}\left[\frac{S^*_{2u}+(1-\epsilon_v)S^*_{2v}}{N^*_2}\right].$$

Appendix II

$$a_{11} = \frac{K_3K_5K_6K_7K_8K_9K_{10}\sigma_1[f_3\sigma_p(1-r)+f_1K_4]+rK_4K_6K_7K_8K_9K_{10}\sigma_1\sigma_p(f_2K_5+f_4\phi_1)}{2\prod_{i=1}^{10}K_i},$$

$$a_{12} = \frac{\sigma_1K_1K_2K_3K_4K_5\left[rg_2K_4K_5\sigma_p+(1-r)g_3K_3K_5\sigma_p+rg_4K_4\phi_1\sigma_p+g_1K_3K_4K_5\right]}{4\prod_{i=1}^{10}K_i},$$

$$a_{21} = \frac{\sigma_2K_6K_7K_8K_9K_{10}\left[qf_6K_9K_{10}\sigma_p+(1-q)f_7K_8K_{10}\sigma_p+qf_8K_9\phi_2\sigma_p+f_5K_8K_9K_{10}\right]}{4\prod_{i=1}^{10}K_i},$$

$$a_{22} = \frac{K_1K_2K_3K_4K_5K_8K_{10}\sigma_2[g_7\sigma_p(1-q)+g_5K_9]+qK_1K_2K_3K_4K_5K_9\sigma_2\sigma_p(g_6K_{10}+g_8\phi_2)}{2\prod_{i=1}^{10}K_i}.$$

$$b_{11} = \frac{K_3K_5K_6K_7K_8K_9K_{10}\sigma_1[\beta_{A_1}\sigma_p(1-r)+\beta_{P_1}K_4]+rK_4K_6K_7K_8K_9K_{10}\sigma_1\sigma_p(\beta_{I_1}K_5+\beta_{H_1}\phi_1)}{2\prod_{i=1}^{10}K_i},$$

$$b_{12} = \frac{\sigma_1K_1K_2K_3K_4K_5\left[r\beta_{I_1}K_4K_5\sigma_p+(1-r)\beta_{A_1}K_3K_5\sigma_p+r\beta_{H_1}K_4\phi_1\sigma_p+\beta_{P_1}K_3K_4K_5\right]}{4\prod_{i=1}^{10}K_i},$$

$$b_{21} = \frac{\sigma_2K_6K_7K_8K_9K_{10}\left[q\beta_{I_2}K_9K_{10}\sigma_p+(1-q)\beta_{A_2}K_8K_{10}\sigma_p+q\beta_{H_2}K_9\phi_2\sigma_p+\beta_{P_2}K_8K_9K_{10}\right]}{4\prod_{i=1}^{10}K_i},$$

$$b_{22} = \frac{K_1K_2K_3K_4K_5K_8K_{10}\sigma_2[\beta_{A_2}\sigma_p(1-q)+\beta_{P_2}K_9]+qK_1K_2K_3K_4K_5K_9\sigma_2\sigma_p(\beta_{I_2}K_{10}+\beta_{H_2}\phi_2)}{2\prod_{i=1}^{10}K_i}.$$

References

[1] "Center for Systems Science and Engineering at Johns Hopkins University. COVID-19," (2020). Online Version

[2] Centers for Disease Control and Prevention, "Coronavirus disease 2019 (COVID-19)," National Center for Immunization and Respiratory Diseases (NCIRD), Division of Viral Diseases (Accessed on March 4, 2020). Online Version

[3] C. N. Ngonghala, E. Iboi, S. Eikenberry, M. Scotch, C. R. MacIntyre, M. H. Bonds, and A. B. Gumel, "Mathematical assessment of the impact of non-pharmaceutical interventions on curtailing the 2019 novel coronavirus," Mathematical Biosciences. **325**, 108364 (2020).

[4] Pfizer, "Pfizer and BioNTech to Submit Emergency Use Authorization Request Today to the U.S. FDA for COVID-19 Vaccine," (2020). Online Version

[5] S. E. Eikenberry, M. Muncuso, E. Iboi, T. Phan, E. Kostelich, Y. Kuang, and A. B. Gumel, "To mask or not to mask: Modeling the potential for face mask use by the general public to curtail the COVID-19 pandemic," Infectious Disease Modeling **5**, 293–308 (2020).

[6] C. N. Ngonghala, E. Iboi, and A. B. Gumel, "Could masks curtail the post-lockdown resurgence of covid-19 in the US?" Mathematical Biosciences **329**, 108452 (2020).

[7] E. A. Iboi, C. N. Ngonghala, and A. B. Gumel, "Will an imperfect vaccine curtail the COVID-19 pandemic in the US?" Infectious Disease Modelling **5**, 510–524 (2020).

[8] National Institute of Health, "Promising Interim Results from Clinical Trial of NIH-Moderna COVID-19 Vaccine," (2020). Online Version

[9] AstraZeneca, "AZD1222 Vaccine Met Primary Efficacy Endpoint in Preventing COVID-19," (2020). Online Version

[10] Graham Lawton, "Everything you Need to Know About the Pfizer/BioNTech COVID-19 Vaccine," (2020). Online Version

[11] Moderna, "Moderna Announces Longer Shelf Life for its COVID-19 Vaccine Candidate at Refrigerated Temperatures," (2020).
Online Version

[12] A. Srivastava and G. Chowell, "Understanding spatial heterogeneity of COVID-19 pandemic using shape analysis of growth rate curves," medRxiv (2020).

[13] K. A. Schneider, G. A. Ngwa, M. Schwehm, L. Eichner, and M. Eichner, "The covid-19 pandemic preparedness simulation tool: Covidsim," BMC Infectious Diseases (2020).

[14] J. Hellewell, S. Abbott, A. Gimma, N. I. Bosse, C. I. Jarvis, T. W. Russell, J. D. Munday, A. J. Kucharski, W. J. Edmunds, F. Sun, et al., "Feasibility of controlling COVID-19 outbreaks by isolation of cases and contacts," The Lancet Global Health **8**, E488–E496 (2020).

[15] A. J. Kucharski, T. W. Russell, C. Diamond, Y. Liu, J. Edmunds, S. Funk, R. M. Eggo, F. Sun, M. Jit, J. D. Munday, et al., "Early dynamics of transmission and control of COVID-19: a mathematical modelling study," The Lancet Infectious Diseases **20**, 553–558 (2020).

[16] L. Xue, S. Jing, J. C. Miller, W. Sun, H. Li, J. G. Estrada-Franco, J. M. Hyman, and H. Zhu, "A data-driven network model for the emerging covid-19 epidemics in Wuhan, Toronto and Italy," Mathematical Biosciences **326**, 108391 (2020).

[17] N. M. Ferguson, D. Laydon, G. Nedjati-Gilani, N. Imai, K. Ainslie, M. Baguelin, S. Bhatia, A. Boonyasiri, Z. Cucunubá, G. Cuomo-Dannenburg, et al., "Impact of non-pharmaceutical interventions (NPIs) to reduce COVID-19 mortality and healthcare demand," London: Imperial College COVID-19 Response Team, March **16** (2020).

[18] H. T. Banks, M. Davidian, J. R. Samuels, and K. L. Sutton, *An Inverse Problem Statistical Methodology Summary*, 249–302 (Springer Netherlands, Dordrecht, 2009).
Online Version

[19] G. Chowell, "Fitting dynamic models to epidemic outbreaks with quantified uncertainty: a primer for parameter uncertainty, identifiability, and forecasts," Infectious Disease Modelling **2**, 379–398 (2017).

[20] C. Zhou, "Evaluating new evidence in the early dynamics of the novel coronavirus COVID-19 outbreak in Wuhan, China with real time domestic traffic and potential asymptomatic transmissions," medRxiv (2020).

[21] N. M. Linton, T. Kobayashi, Y. Yang, K. Hayashi, A. R. Akhmetzhanov, S.-m. Jung, B. Yuan, R. Kinoshita, and H. Nishiura, "Incubation period and other epidemiological characteristics of 2019 novel coronavirus infections with right truncation: a statistical analysis of publicly available case data," Journal of Clinical Medicine **9**, 538 (2020).

[22] World Health Organization, "Coronavirus disease 2019 (COVID-19): situation report, 46," WHO (2020).

[23] Z. Wu and J. M. McGoogan, "Characteristics of and important lessons from the coronavirus disease 2019 (COVID-19) outbreak in China: summary of a report of 72 314 cases from the Chinese Center for Disease Control and Prevention," JAMA (2020).

[24] S. Kissler, C. Tedijanto, E. Goldstein, Y. Grad, and M. Lipsitch, "Projecting the transmission dynamics of SARS-CoV-2 through the postpandemic period," Science (2020).
Online Version

[25] L. Zou, F. Ruan, M. Huang, L. Liang, H. Huang, Z. Hong, J. Yu, M. Kang, Y. Song, J. Xia, et al., "SARS-CoV-2 viral load in upper respiratory specimens of infected patients," New England Journal of Medicine **382**, 1177–1179 (2020).

[26] V. Lakshmikantham and A. Vatsala, "Theory of differential and integral inequalities with initial time difference and applications," in "Analytic and Geometric Inequalities and Applications," 191–203 (Springer, 1999).

[27] H. W. Hethcote, "The mathematics of infectious diseases," SIAM Review **42**, 599–653 (2000).

[28] P. van den Driessche and J. Watmough, "Reproduction numbers and sub-threshold endemic equilibria for compartmental models of disease transmission," Mathematical Biosciences **180**, 29–48 (2002).

[29] O. Diekmann, J. A. P. Heesterbeek, and J. A. Metz, "On the definition and the computation of the basic reproduction ratio R_0 in models for infectious diseases in heterogeneous populations," Journal of Mathematical Biology **28**, 365–382 (1990).

[30] R. M. Anderson and R. M. May, "Vaccination and herd immunity to infectious diseases," Nature **318**, 323–329 (1985).

[31] R. M. Anderson, "The concept of herd immunity and the design of community-based immunization programmes," Vaccine **10**, 928–935 (1992).

[32] D. Bernoulli, "Essai d'une nouvelle analyse de la mortalité causée par la petite vérole, et des avantages de l'inoculation pour la prévenir," Histoire de l'Acad., Roy. Sci. 1–45 (1760).

[33] R. Ross, *The prevention of malaria* (John Murray, 1911).

[34] W. O. Kermack and A. G. McKendrick, "A contribution to the mathematical theory of epidemics," Proceedings of the Royal Society of London. Series A, Containing papers of a mathematical and physical character **115**, 700–721 (1927).